J Nanopart Res (2010) 12:1187–1196
DOI 10.1007/s11051-009-9749-0

RESEARCH PAPER

Synthesis of magnetic core–shell Fe_3O_4–Au nanoparticle for biomolecule immobilization and detection

Uğur Tamer · Yusuf Gündoğdu · İsmail Hakkı Boyacı · Kadir Pekmez

Received: 10 February 2009 / Accepted: 28 August 2009 / Published online: 17 September 2009

Abstract The production of monodispersed magnetic nanoparticles with appropriate surface modification has attracted increasing attention in biomedical applications including drug delivery, separation, and purification of biomolecules from the matrices. In the present study, we report rapid and room temperature reaction synthesis of gold-coated iron nanoparticles in aqueous solution using the borohydride reduction of $HAuCl_4$ under sonication for the first time. The resulting nanoparticles were characterized with transmission electron microscopy (TEM), electron spectroscopy for chemical analysis (ESCA), ultraviolet visible spectroscopy (UV–Vis), and X-ray diffraction (XRD). Surface charges and magnetic properties of the nanoparticles were also examined. The pattern of Fe_3O_4 nanoparticles is face centered cubic with an average diameter of 9.5 nm and the initial reduction of gold on the surface of Fe_3O_4 particles exhibits uniform Fe_3O_4–Au nanoparticles with an average diameter of 12.5 nm. The saturation magnetization values for the uncoated and gold-coated Fe_3O_4 nanoparticles were found to be 30 and 4.5 emu/g, respectively, at 300 K. The progression of binding events between boronic acid terminated ligand shell and fructose based on the covalent bonding interaction was measured by absorbance spectral changes. Immunomagnetic separation was also performed at different *E. coli* concentration to evaluate capturing efficiency of resulting nanoparticles. Immunomagnetic separation percentages were varied in a range of 52.1 and 21.9% depend on the initial bacteria counts.

Keywords Magnetic nanoparticles · Gold–iron oxide nanoparticle · Immunomagnetic separation · Boronic acid · *E. coli* · Composite nanomaterials · Nanomedicine

U. Tamer (✉) · Y. Gündoğdu
Department of Analytical Chemistry, Faculty of Pharmacy, Gazi University, 06330 Ankara, Turkey
e-mail: utamer@gazi.edu.tr

İ. H. Boyacı
Department of Food Engineering, Hacettepe University, Beytepe, Ankara, Turkey

K. Pekmez
Department of Chemistry, Hacettepe University, Beytepe, Ankara, Turkey

Introduction

Magnetic nanoparticles have attracted broad attention due to their potential applications in magnetic resonance imaging (NMR; Weissledel et al. 2000; Seo et al. 2006; Lee et al. 2007), data storage (Sun et al. 2000), drug delivery (Chouly et al. 1996; Storm et al. 1995; Zhang et al. 2002; Yamazaki and Ito 1990; Widder et al. 1980). Numerous research works have been performed to evaluate the use of magnetic nanoparticles in the treatment of carcinogenic brain

tumor cells and breast cancer cells (Subramani et al. 2009). Gold nanoparticles, liposomes, and polymeric micelle platforms have also been tested as drug delivery systems to target tumor cells and deliver anticarcinogenic drug in a controlled manner (Hosseinkhani and Hosseinkhani 2009; Hosseinkhani and Tabata 2006; Hosseinkhani 2006; Hosseinkhani et al. 2008). Important progress has also been made in biomedical applications including separation and purification of biomolecules from the matrices (Xu et al. 2006; Meldrum et al. 1992; Tanaka and Matsunaya 2000).

It would be advantageous to synthesize monodisperse magnetic nanoparticles in many applications, because different magnetization properties could be observed when the polydisperse magnetic nanoparticles used (Gupta and Gupta 2005). However, the production of monodispersed, nanometer-sized magnetic particles remains a significant challenge and numerous method has been reported including reduction at high temperature, borohydride reduction of ferrous salts, or thermal decomposition of $Fe(CO)_5$ (Chen and Nikles 1999; Chamberlin et al. 2002). The wet chemical synthesizing routes for magnetic nanoparticles are simple and the control of size, shape, and composition of nanoparticles depends on the type of salts used, Fe^{+2} and Fe^{+3} ratio, pH, and ionic strength of the media (Gupta and Gupta 2005). To achieve high magnetization and providing well-known chemical surfaces with various functional groups for coupling, heterodimers of nanoparticles which are composed of magnetic and semiconductor colloids (Gu et al. 2004) and supermagnetic polystyrene microsphere for immunity separation (Ugelstad et al. 1980) was prepared. Coating the particle surface with a silica layer was also achieved, however, significant reduction in magnetization was observed due to the decrease of the magnetite fraction in each microsphere (Lu et al. 2002). Fe_3O_4/polystyrene/silica nanosphere via combined miniemulsion–emulsion polymerization was also developed (Xu et al. 2006).

The well-known surface chemistry of gold has been proven that it exhibits good surface for subsequent functionalization and it may provide not only the stability to the magnetic nanoparticles in solution but also helps in binding the various chemical and biological agents (Lin et al. 2001; Cho et al. 2005; Mikhaylova et al. 2004; Mandal et al. 2005; Lyon et al. 2004; Wang et al. 2005a, b). Extensive investigations involving gold nanoparticles as nanoscale materials and devices are currently underway and there are many synthetic methods to make gold nanoparticles (Brown and Hutchison 1997, 1999; Warner et al. 2000; Weare et al. 2000; Yonezawa et al. 2001; Zhao et al. 1998). The most common approach involves citrate or borohydride reduction of a gold salt to produce gold nanoparticles (Cho et al. 2005; Lin et al. 2001; Pham et al. 2008). However, chemical reduction of auric and ferrous salts is problematic in a one-pot synthesis condition because metallic gold will be nucleate particles or aggregate before iron from the salt solution (Chen et al. 2003). Carpenter reported that gold-coated iron nanoparticles were formed inside the reverse micelle by the reduction of a metal salt using sodium borohydride (Carpenter 2001; Carpenter et al. 2000; Lin et al. 2001). Zhou et al. (2001) prepared gold-coated iron nanoparticle using reverse micelles characterized by transmission electron microscopy (TEM). The formation of gold shell on the magnetic nanoparticle was also performed by an iterative reduction method using hydroxylamine as a reductant (Jeong et al. 2006). The optical and magnetic properties of the fluorescent silica-coated gold nanorods and magnetic nanocrystals were also reported (Heitsch et al. 2008).

Up to now, applications of gold-coated magnetic nanoparticles are relatively rare. This might be caused by the difficulties in synthesizing procedures such as heating, time consuming as well as the needs for a specific chemical modification to prevent aggregation. Here, we report rapid and room temperature reaction synthesis of gold-coated Fe_3O_4 in aqueous solution using the borohydride reduction of $HAuCl_4$ under sonication for the first time and subsequent recognition of the target provide an effective means for separation via application of an applied magnetic field. The two-step synthetic method was carried out. First, iron nanoparticles were synthesized and then resulting iron nanoparticles were-coated with gold using the borohydride reduction of $HAuCl_4$ under sonication. Sonication procedure was applied to give better particle monodispersity and to avoid agglomeration problems associated with ionic interactions. The resulting nanoparticles were characterized with TEM, electron spectroscopy for chemical analysis (ESCA), ultraviolet visible spectroscopy (UV–Vis), and X-ray diffraction (XRD). Surface charges and magnetic properties of the nanoparticles were also

examined. Mercaptopropionic acid derivatized gold iron nanoparticles used as a scaffold for further stepwise modification, leading to a boronic acid terminated ligand shell. The progression of binding events between boronic acid terminated ligand shell and fructose based on the covalent bonding interaction was measured by absorbance spectral changes. Immunomagnetic separation was also performed at different *Escherichia coli* concentration to evaluate capturing efficiency of resulting nanoparticles.

Experimental section

General

All chemicals were obtained from commercial sources and used as received. $FeSO_4 \cdot 7H_2O$, sodium hydroxide, hydrogen peroxide, and sulfuric acid were purchased from Merck. Hydrogen tetrachloroaurate (III) hydrate, sodium borohydride, 3-aminophenylboronic acid, $FeCl_3$, *N*-Ethyl-*N*′-(3-dimethylaminopropyl)-carbodiimide (EDC), sodium phosphate monobasic, and sodium phosphate dibasic were purchased from Sigma-Aldrich. *N*-hydroxysuccinimide (NHS) was obtained from Fluka. Commercial streptavidin-coated paramagnetic beads of $\sim$1.0 μm in diameter and mono-dispersed suspension of 6.7×10^8 beads/mL were purchased from Dynal Inc. (Great Neck, NY, USA). Biotin-conjugated rabbit antibody to *E. coli* was obtained from Abcam plc (Ampridge, UK). *E. coli* K12 strain was supplied from Refik Saydam National Type Culture Collections, Ankara, Turkey. Sorbitol MacConkey Agar and Tryptic Soy Broth were obtained from Merck KGaA. Na_2HPO_4 and KH_2PO_4 were obtained from J.T.BAKER, used as PBS. MilliQ water (Millipore) was used throughout. All buffer solutions were prepared to 0.1 M concentration at pH 7. Aqua regia solution (1:3 nitric acid/hydrochloric acids) was used to clean quartz cuvettes and the glassware used to synthesize the nanoparticles.

Optical absorption spectroscopy measurements were performed in a Spectronics, Genesis model single beam spectrophotometer using 1 cm path length quartz cuvettes. Spectra were collected within a range of 300–800 nm. TEM measurements were performed on a JEOL instrument. TEM samples were prepared by pipetting 10 μL of nanoparticle solution onto TEM grids and allowed to stand for 10 min. XRD measurements were performed on a Philips PW-1140 model diffractometer with Cu $K\alpha$ radiation at a wavelength of 1.5406 Å. Calculation by Scherrer equation determined the crystallite sizes of nanoparticles. The measurements of zeta potential and hydrodynamic diameter were carried out using Malvern Instrument Zetasizer. ESCA data were obtained using a Specs ESCA (Berlin, Germany) system with a dual anode (Mg/Al) X-ray source and EA 200 hemispherical electrostatic energy analyzer equipped with multichannel detector (MCD) with 18 discrete channels. The X-ray beam was generated with an unmonochromatized Mg $K\alpha$ source operated at 15 kV and 100 W and the observed binding energies were calculated with reference to the saturated hydrocarbon peak at 284.6 eV.

Synthesis of iron nanoparticles

The Fe_3O_4 nanoparticles were prepared by coprecipitation of Fe(II) and Fe(III). Fe(II)/Fe(III) ratio is kept as 0.5 in an alkaline solution. Briefly, 1.28 M $FeCl_3$ and 0.64 M $FeSO_4 \cdot 7H_2O$ were dissolved in deionized water. The solution was then stirred vigorously until the iron salts were dissolved. Subsequently, a solution of 1 M NaOH was added dropwise into the mixture with stirring for 40 min. Precipitated magnetite is black in color. The chemical reaction of Fe_3O_4 precipitation may be written as follows (Gupta and Gupta 2005)

$$Fe^{+2} + 2Fe^{+3} + 8OH^- \rightarrow Fe_3O_4 + 4H_2O.$$

The black precipitate was collected on a permanent magnet and washed with deionized water. To obtain oxidized Fe_3O_4 nanoparticles, the resulting iron salts precipitate were first washed in 2 M $HClO_4$ and were waited for 3 h to oxidize iron salts to Fe_3O_4 until the color of particle become brown under argon atmosphere. The particles were then centrifuged for 20 min at 10,000 rpm. Subsequently, supernatant solution is discarded and washed with deionized water. Washing procedure was performed three times.

Synthesis of gold-coated Fe_3O_4 nanoparticles

Au shell coating procedure was carried out in a sonicator in order to encapsulate the iron nanoparticles with gold shells. Approximately, 5×10^{13} iron oxide particles suspended in aqueous solution of

0.5 mL 0.01 M $HAuCl_4$ and stirred in a sonication for 2 min. The reaction solution containing magnetic cores and reduction agent 0.01 M $NaBH_4$ (prepared in cold water approximately 4 °C) was sonicated for 5 min then the sonication was stopped. Resulting nanoparticle solution color is dark red.

Usability of Fe_3O_4–Au nanoparticles in bioassay

Usability of developed core–shell nanoparticles were investigated in two different bioassay applications. They were fructose measurement based on boronic acid-activated magnetic nanoparticles and immunomagnetic separation of *E. coli* using developed core–shell nanoparticles. Boronic acid terminal groups were introduced with the following steps. Briefly, gold–iron nanoparticle was transferred into the ethanol solution and was degassed with argon gas before use. Then, 230 mM 3-mercaptopropionic acid solution was added and the final mixture was allowed to stand for 4 h in order to allow for 3-mercaptopropionic acid to be chemisorbed onto the gold iron nanoparticles. Unreacted excess 3-mercaptopropionic acid was removed from the alkanethiol-modified nanoparticles by applying a permanent magnet for 30 min followed by decantation of supernatants and resuspension in ethanol. This procedure was repeated for a minimum of three times. To prevent light-induced flocculation of the colloids and oxidation of the alkanethiolates, all nanoparticles solutions were stored in the dark and refrigerated at 4 °C (Lee and Perez Luna 2005). To form boronic acid terminal group, a 1:1 mixture of 4 mM NHS and 4 mM EDC was reacted with 3-mercaptopropionic acid-modified gold iron nanoparticle solutions for 40 min. This step produces colloidal gold iron particle with NHS ester groups on the nanoparticle surface (Kalinin et al. 1995; Chilkoti and Stayton 1995). Unreacted NHS-EDS was removed from the resulting gold iron nanoparticle solutions by a magnet and resuspension in phosphate buffer (pH 7). After this procedure, 10 mM boronic acid in buffer solution was added and reacted for 3 h to form boronic acid terminal groups on the iron gold particles. Unreacted excess boronic acid was removed by a magnet and resuspension as described above. Fructose binding on the gold iron nanoparticle was investigated by monitoring the UV–Vis spectra of gold-modified iron nanoparticles. Fructose solution was added to the 100 mM carbonate buffer solution at pH 11 including gold iron oxide nanoparticles.

For the immunomagnetic separation of *E. coli*, the streptavidin-coated commercial paramagnetic microbeads (10 μL) were added into a tube containing biotin-conjugated antibodies (10 μL, 0.2 mg mL^{-1}), and then the tube was shaken on a vortex mixer (Stuart, UK) at room temperature for 20 min. The beads were coated with antibodies and removed magnetically form the solution and washed 3 times by resuspending them in PBS (pH 7.5, 0.1 M). EDC/NSH-activated core–shell nanoparticles were used for preparation of antibodies-coated paramagnetic nanoparticle. Similar with the commercial beads, activated nanoparticles were mixed with antibody, incubated and then antibody-coated nanoparticles were removed from solution by magnetically and washed with PBS. Antibody unbounded active sides of nanoparticles were blockaded by incubation of antibody-coated nanoparticles with 10 μL of ethanolamine solution at room temperature for 20 min. Immunomagnetic separation was performed at three different *E. coli* concentration (10^2, 10^3, 10^4 cfu mL^{-1}) to visualize the effect of initial bacteria count on capturing efficiency. Antibody-coated beads (10 μL) were mixed with *E. coli* solution (250 μL) and incubated at room temperature on the vortex mixer for 30 min. After incubation, captured bacteria were removed by magnetically and 100 μL supernate solution containing uncaptured *E. coli* were plated on Sorbitol MacConkey Agar and incubated at 37 °C for 24 h. *E. coli* colonies were counted to determine the percentage of the captured *E. coli.* Two measurements were performed and the average of the measurement was used for calculation of the immunomagnetic separation percentage.

Results and discussion

Characterization of nanoparticles

Aqueous magnetic nanoparticle preparation could be facile and easy for conjugation in aqueous solution. In addition, for the preparation of gold iron nanoparticles in aqueous solution seems to be a convenient candidate for various applications, since surface modification could be performed through well-known thiol chemistry. For the preparation of the gold

coating, initial experiments were performed by direct reduction of gold (III) in the presence of Fe_3O_4 nanoparticles. After the reduction, the morphology of the gold iron nanoparticles was not uniform, formation of large cluster, and particle agglomeration resulting in increased particle size were observed.

In order to stabilize and to obtain smoother and homogenous gold layer, gold precursor ions were directly reduced by sodium borohydride with the aid of ultrasonic agitation. Sonication procedure was applied to give better particle monodispersity and to avoid agglomeration problems associated with ionic interactions and corresponding polydispersity index (PDI) of gold-coated iron nanoparticles was 0.39. After coating gold layer to the iron nanoparticle, zeta potential value is decreased from 19.3 to 3.57 mV. The change in the zeta potential of iron nanoparticles is due to the gold coating. Resulting gold iron nanoparticles were separated from the gold nanoparticles by a magnet. Dynamic light scattering measurements showed that the mean hydrodynamic diameter of Fe_3O_4 and Fe_3O_4–Au nanoparticles was found to be 100 and 122 nm, respectively. The light scattering measurements does not give true size of nanoparticles. Figure 1 shows the morphology of typical iron oxide nanoparticles prior to gold coating. Fe_3O_4 nanoparticles were synthesized in wet chemical method yielded nanometer-sized Fe_3O_4 particles with an average diameter of 9.5 ± 3 nm, as determined from TEM images. The pattern of magnetic nanoparticles is face centered cubic as shown in Fig. 1.

Figure 2 indicated the TEM image of Fe_3O_4–Au nanoparticles. The particles after coating with gold appear much darker than the Fe_3O_4 nanoparticles because gold is much more electron dense than iron oxide and this observation is consistent with previous report (Stuart et al. 2005). After these reduction processes, TEM analysis reveals that average particle

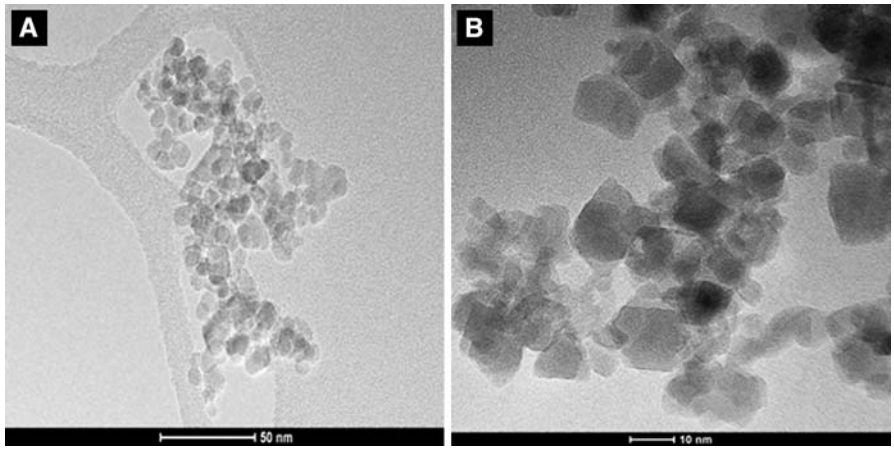

Fig. 1 TEM images of Fe_3O_4 nanoparticles

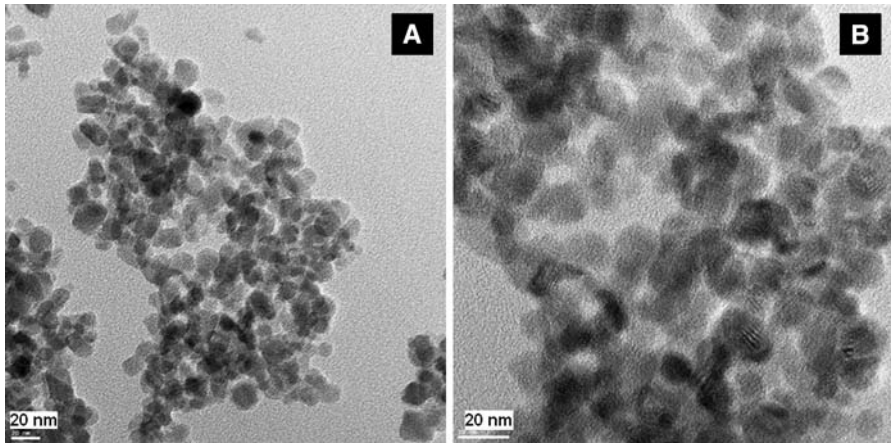

Fig. 2 TEM images of Fe_3O_4–Au nanoparticles

diameter is increased from 9.5 to 12.5 nm. The initial reduction of gold on the surface of face centered cubic iron oxide particles exhibits uniform gold iron nanoparticles with an average diameter 12.5 ± 3 nm. In addition, TEM micrographs of the gold iron nanoparticle material show that iron gold nanoparticles appear clustered with non-capped iron nanoparticles. Iron nanoparticles appear dispersed and do not cluster when they are not coated with gold. This is a result of the attachment of iron particles to gold iron nanoparticles together.

The crystalline structure of Fe_3O_4 and core/shell Fe_3O_4/Au nanoparticles were further examined with XRD. Figure 3 indicates the XRD pattern of synthesized Fe_3O_4 nanoparticles. All the reflections correspond to Fe_3O_4 (JCPDS 11-614). The face centered cubic was observed as the pattern of iron nanoparticles. As labeled in Fig. 3b, the peaks at 38.14°, 44.36°, 64.58° are assigned to the Au–Fe position of (111), (200), (220), which are located in the positions of the corresponding materials (JCPDS card No: 04-0784). The crystalline structure of gold iron nanoparticles has proven that the particles are face centered cubic with the dominant crystal planes of 111. In addition, the average crystalline size of as synthesized Fe_3O_4 and gold-coated Fe_3O_4 nanoparticles can be estimated as 7.4 and 10.5 nm, respectively.

Magnetic particles may exhibit different magnetic properties due to their synthetic conditions (Gupta and Gupta 2005). The gold-coated iron nanoparticles were superparamagnetic at room temperature and the saturation magnetization values as great as 60 emu/g have been reported (Pham et al. 2008; Xu et al. 2007, 2008; Ban et al. 2005). The hysteresis loop measured for the uncoated and gold-coated Fe_3O_4 nanoparticles is shown in Fig. 4. As can be seen, the typical characteristics of superparamagnetic behavior are observed. The saturation magnetization values from the magnetization curve in Fig. 4 for the uncoated and gold-coated Fe_3O_4 nanoparticles were found to be 30 and 4.5 emu/g, respectively, at 300 K. The decrease of saturated magnetization was attributed to the formation of the gold layer.

Applications of developed core–shell nanoparticles

The binding properties and the separation ability of the gold shell of the nanoparticles were investigated. The location of the extinction maximum of gold nanoparticles is highly dependent on the dielectric properties of the surrounding environment and that

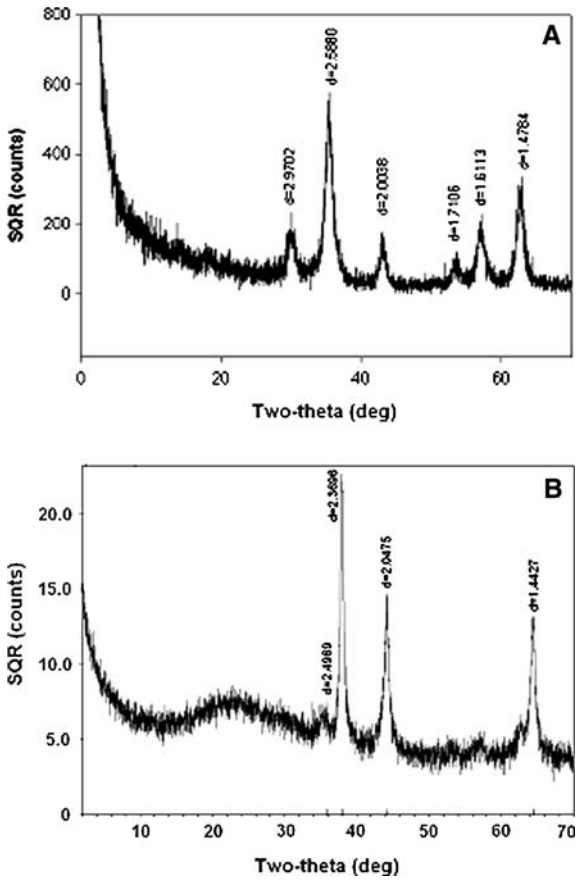

Fig. 3 XRD pattern of **a** Fe_3O_4 and **b** Fe_3O_4–Au nanoparticles

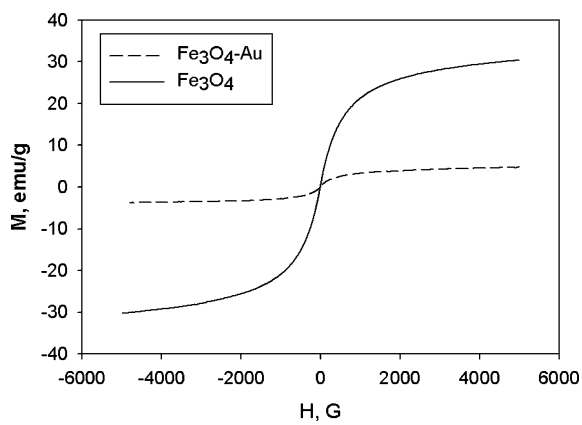

Fig. 4 Hysteresis loops of Fe_3O_4 (*solid line*) and Fe_3O_4–Au (*dotted line*) nanoparticles

wavelength shifts in the extinction maximum of nanoparticles can be used to detect molecule-induced changes surrounding the nanoparticles (Stuart et al. 2005). The interaction of boronic acid and saccharide has attracted many attentions, which has been used to detect polyols such as glucose and catechol (Mader and Wolfbeis 2008). In the present study, fructose is selected for target saccharide. For this purpose, the Fe_3O_4–Au nanoparticles can be fully dispersed in ethanol solution and the magnetic properties and utility of gold iron nanoparticles were performed by the magnetic separation of attached 3-phenylboronic acid on the gold shell.

The formation of the gold iron nanoparticle and subsequent attachment by boronic acid for the binding of fructose was illustrated in Fig. 5. The specific reactivity between 3-mercaptopropionic acid-modified gold iron nanoparticle and 3-aminophenylboronic acid is clearly evidenced by the gradual decrease of the surface plasmon resonance band at 550 nm and its expansion to the longer wavelength as shown in Fig. 5. The interaction of the 3-aminophenylboronic acid-modified gold iron nanoparticle with fructose was assessed with optical absorption spectroscopy. Phenylboronic acid-modified gold iron nanoparticle show an absorption peak at 580 nm that experiences significant red shifting and broadening. This result shows the fructose particle interaction. To verify and confirm the surface modification, XPS measurements were also carried. As is seen from XPS spectrum in Fig. 6, 3-aminophenylboronic acid modification is successful.

To further demonstrate the viability of the gold iron nanoparticles for magnetic bioseparation, the following proof-of-concept demonstration experiment exploits both the magnetic core and the bioaffinity of the gold shell. In this experiment, the gold-based surface protein binding reactivity and the magnetic separation capability were examined. Mercaptopropionic acid-modified gold iron nanoparticles were coupled to the antibody via covalent coupling, forming antibody immobilized Fe_3O_4–Au nanoparticles. The antibody immobilized Fe_3O_4 nanoparticles were reacted with *E. coli*. The magnetic separation of these nanoparticles was easily accomplished and gold iron nanoparticles were separated only by a magnet. Results from control experiments were also included for comparison in which the commercial macromagnetic particles were used to replace the Fe_3O_4–Au nanoparticles. IMS percentages were varied in a range of 52.1 and 21.9% depend on the initial bacteria counts.

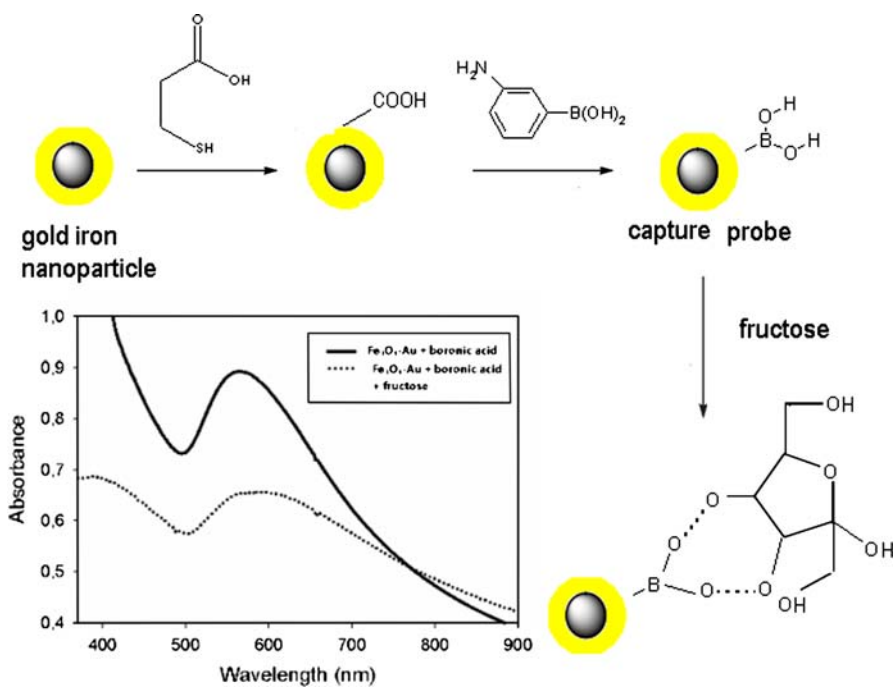

Fig. 5 Schematic illustration of the functionalized nanoparticles formation process and UV–Vis spectra of boronic acid-modified Fe_3O_4–Au nanoparticles after interaction of the 3-aminophenylboronic acid-modified gold iron nanoparticle with fructose

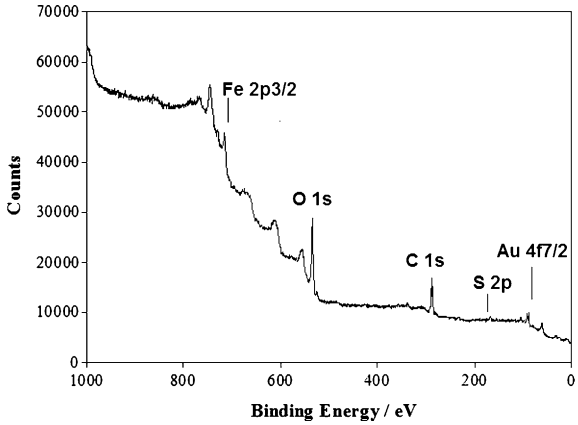

Fig. 6 Wide scan XPS spectrum of boronic acid-modified Fe_3O_4–Au nanoparticles

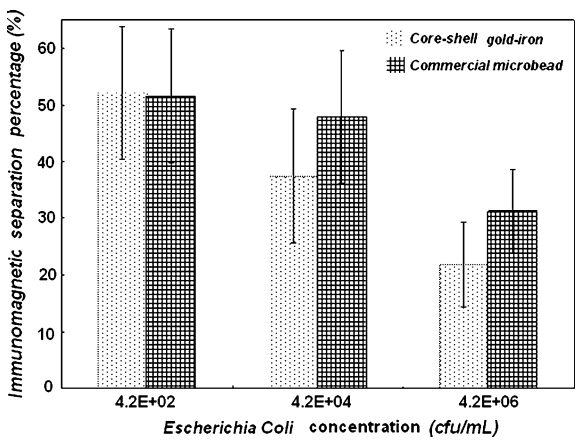

Fig. 7 Comparison of magnetic bioseparation using gold–iron nanoparticles and commercial macromagnetic particles

The results indicated that the nanoparticle developed in this study was as good as commercial particle for bacteria separation as shown in Fig. 7. IMS percentage for both particles was decreased when the initial bacteria concentration was increased. It means that the number of particles in separation medium became insufficient when the initial bacteria concentration was increased. Biological entity adhesion to the surface of nanoparticle could be also mediated by different physicochemical interactions including Van der Waals, electrostatic, and acid–base interactions (Hosseinkhani et al. 2003). It is likely that *E. coli* interacts with the antibody on the surface of nanoparticles due to high affinity and possible interaction between bacteria and magnetic Fe_3O_4–Au nanoparticles could be antibody–antigen.

Conclusions

Isolation of target molecule or organism from sample solution is one of the important issues in most of the bioassay studies. Micro particles commonly used for this purpose and usage of micro particles has some limitation in bioassay. Some of the limitations could be eliminated by using magnetic nanoparticles. High surface area of the nanoparticles gives an opportunity to minimize steric hindrance problem, increase the immuno capturing efficiency and reaction efficiencies performed on particle surface. We present findings of the fabrication and characterization of gold-coated iron oxide nanoparticles. The magnetic core and gold shell have proven that resulting nanoparticle is viable for determination and magnetic bioseparation. The modification of gold iron nanoparticles through thiol chemistry seems to be advantageous in that it could be used to link the nanoparticles with diverse biomolecules. Fructose assay performed in this study demonstrated that the particle gives an opportunity of detection of small molecule on particle surface and it is possible to use magnetic nanoparticles to separate micro size bacteria in sample medium with higher performance rather then magnetic micro particles.

Acknowledgment The authors are grateful for the financial supports provided by The Scientific and Technological Research Council of Turkey; Project Number: 107T682.

References

Ban Z, Barnaov YA, Li F, Golup VO, O'Conner CJ (2005) The synthesis of core shell iron@gold nanoparticles and their characterization. J Mater Chem 15:4660–4662

Brown LO, Hutchison JE (1997) Convenient preparation of stable, narrow-dispersity, gold nanocrystals by ligand exchange reactions. J Am Chem Soc 119(50):12384–12385

Brown LO, Hutchison JE (1999) Controlled growth of gold nanoparticles during ligand exchange. J Am Chem Soc 121(4):882–883

Carpenter EE (2001) Iron nanoparticles as potential magnetic carriers. J Magn Magn Mater 225(1–2):17–20

Carpenter EE, Kumbhar A, Wiemann JA, Srikanth H, Wiggins J, Zhou W et al (2000) Synthesis and magnetic properties of gold-iron-gold nanocomposites. Mater Sci Eng A 286(1):81–86

Chamberlin RV, Humfeld KD, Farrell D, Yamamuro S, Ijiri Y, Majetich SA (2002) Magnetic relaxation of iron nanoparticles. J Appl Phys 91(10):6961–6963

Chen M, Nikles DE (1999) Chain-of-cubes iron nanoparticles prepared by borohydride reduction of acicular akaganeite particles. J Appl Phys 85(8):5504–5506

Chen M, Yamamuro S, Farrell D, Majetich SA (2003) Gold-coated iron nanoparticles for biomedical applications. J Appl Phys 93(10):7551–7553

Chilkoti A, Stayton PS (1995) Molecular-origins of the slow streptavidin-biotin dissociation kinetics. J Am Chem Soc 117(43):10622–10628

Cho SJ, Idrobo JC, Olamit J, Liu K, Browning ND, Kauzlarich SM (2005) Growth mechanisms and oxidation resistance of gold-coated iron nanoparticles. Chem Mater 17(12):3181–3186

Chouly C, Pouliquen D, Lucet I, Jeune JJ, Jallet P (1996) Development of superparamagnetic nanoparticles for MRI: effect of particle size, charge and surface nature on biodistribution. J Microencapsul 13(3):245–255

Gu HW, Zheng R, Zhang X, Xu B (2004) Facile one-pot synthesis of bifunctional heterodimers of nanoparticles: a conjugate of quantum dot and magnetic nanoparticles. J Am Chem Soc 126(18):5664–5665

Gupta AK, Gupta M (2005) Synthesis and surface engineering of iron oxide nanoparticles for biomedical applications. Biomaterials 26(18):3995–4021

Heitsch AT, Smith DK, Patel RN, Ress D, Korgel BA (2008) Multifunctional particles: magnetic nanocrystals and gold nanorods coated with fluorescent dye-doped silica shells. J Solid State Chem 181(7):1590–1599

Hosseinkhani H (2006) DNA nanoparticles for gene delivery to cells and tissue. Int J Nanotechnol 3(4):416–461

Hosseinkhani H, Hosseinkhani M (2009) Biodegradable polymer-metal complexes for gene and drug delivery. Curr Drug Saf 4(1):79–83

Hosseinkhani H, Tabata Y (2006) Self assembly of DNA nanoparticles with polycations for the delivery of genetic materials into cells. J Nanosci Nanotechnol 6(8):2320–2328

Hosseinkhani H, Aoyamaa T, Ogawab O, Tabataa Y (2003) Tumor targeting of gene expression through metal-coordinated conjugation with dextran. J Control Release 88:297–312

Hosseinkhani H, Hosseinkhani M, Gabrielson NP, Pack DW, Khademhosseini A, Kobayashi H (2008) DNA nanoparticles encapsulated in 3D tissue-engineered scaffolds enhance osteogenic differentiation of mesenchymal stem cells. J Biomed Mater Res A 85:47–60

Jeong J, Ha TH, Chung BH (2006) Enhanced reusability of hexa-arginine-tagged esterase immobilized on gold-coated magnetic nanoparticles. Anal Chim Acta 569(1–2): 203–209

Kalinin NL, Ward LD, Winzor DJ (1995) Effects of solute multivalence on the evaluation of binding constants by biosensor technology-studies with concanavalin-a and interleukin-6 as partitioning proteins. J Anal Biochem 228(2):238–244

Lee S, Perez Luna VH (2005) Dextran-gold nanoparticle hybrid material for biomolecule immobilization and detection. Anal Chem 77(22):7204–7211

Lee JH, Huh YM, Jun YW, Seo JW, Jang JT, Song HT et al (2007) Artificially engineered magnetic nanoparticles for ultra-sensitive molecular imaging. Nat Med 13(1):95–99

Lin J, Zhou W, Kumbhar A, Wiemann J, Fang J, Carpenter EE et al (2001) Gold-coated iron (Fe@Au) nanoparticles: synthesis, characterization, and magnetic field-induced self-assembly. J Solid State Chem 159(1):26–31

Lu Y, Yin YD, Mayers BT, Xia YN (2002) Modifying the surface properties of superparamagnetic iron oxide nanoparticles through a sol-gel approach. Nano Lett 2(3):183–186

Lyon JL, Fleming DA, Stone MB, Schiffer P, Williams ME (2004) Synthesis of Fe oxide core/Au shell nanoparticles by iterative hydroxylamine seeding. Nano Lett 4(4): 719–723

Mader HS, Wolfbeis OS (2008) Boronic acid based probes for microdetermination of saccharides and glycosylated biomolecules. Microchim Acta 162(1–2):1–34

Mandal M, Kundu S, Ghosh SK, Panigrahi S, Sau TK, Yusuf SM et al (2005) Magnetite nanoparticles with tunable gold or silver shell. J Colloid Interface Sci 286(1):187–194

Meldrum FC, Heywood BR, Mann S (1992) Magnetoferritin—in vitro synthesis of a novel magnetic protein. Science 257(5069):522–523

Mikhaylova M, Kim DK, Bobrysheva N, Osmolowsky M, Semenov V, Tsakalatos T et al (2004) Superparamagnetism of magnetite nanoparticles: dependence on surface modification. Langmuir 20(6):2472–2477

Pham TTH, Cao C, Sim SJ (2008) Application of citrate-stabilized gold coated ferric oxide composite nanoparticles for biological separations. J Magn Magn Mater 320:2049–2055

Seo WS, Lee JH, Sun XM, Suzuki Y, Mann D, Liu Z, Terashima M, Yang PC, Mcconnell MV, Niohimura DG, Dai HJ (2006) FeCo/graphitic-shell nanocrystals as advanced magnetic-resonance-imaging and near-infrared agents. Nat Mater 5(12):971–976

Storm G, Belliot SO, Daemen T, Lasic DD (1995) Surface modification of nanoparticles to oppose uptake by the mononuclear phagocyte system. Adv Drug Deliv Rev 17(1):31–48

Stuart DA, Haes AJ, Yonzon CR, Hicks EM, Van Duyne RP (2005) Biological applications of localised surface plasmonic phenomenae. IEE Proc Nanobiotechnol 152(1):13–32

Subramani K, Hosseinkhani H, Khraisat A, Hosseinkhani M, Pathak Y (2009) Targeting nanoparticles as drug delivery systems for cancer treatment. Curr Nanosci 5(2):134–140

Sun SH, Murray CB, Weller D, Folks L, Moser A (2000) Monodisperse FePt nanoparticles and ferromagnetic FePt nanocrystal superlattices. Science 287(5460):1989–1992

Tanaka T, Matsunaya T (2000) Fully automated chemiluminescence immunoassay of insulin using antibody-protein A-bacterial magnetic particle complexes. Anal Chem 72(15):3518–3522

Ugelstad J, Mork PC, Kaggerud KH, Ellingsen T, Berge A (1980) Swelling of oligomer-polymer particles. New methods of preparation of emulsions and polymer dispersions. Adv Colloid Interface Sci 13(1–2):101–140

Wang LY, Luo J, Maye MM, Fan Q, Rendeng Q, Engelhard MH et al (2005a) Iron oxide-gold core-shell nanoparticles and thin film assembly. J Mater Chem 15(18):1821–1832

Wang LY, Luo J, Fan Q, Suzuki M, Suzuki IS, Engelhard MH, Lin YH, Kim N, Wang JQ, Zhong CJ (2005b) Monodispersed core-shell Fe_3O_4@Au nanoparticles. J Phys Chem B 109(46):21593–21601

Warner MG, Reed SM, Hutchision JE (2000) Small, water-soluble, ligand-stabilized gold nanoparticles synthesized by interfacial ligand exchange reactions. Chem Mater 12(11):3316–3320

Weare WW, Reed SM, Warner MG, Hutchison JE (2000) Improved synthesis of small (d(CORE) approximate to 1.5 nm) phosphine-stabilized gold nanoparticles. J Am Chem Soc 122(51):12890–12891

Weissledel R, Moure A, Mahmood U, Bhorade R, Benveniste M, Chiocca E et al (2000) In vivo magnetic resonance imaging of transgene expression. Nat Med 6(3):351–355

Widder KJ, Senge AE, Ranney DF (1980) Invitro release of biologically-active adriamycin by magnetically responsive albumin microspheres. Cancer Res 40(10):3512–3517

Xu H, Cui L, Tong N, Gu H (2006) Development of high magnetization Fe_3O_4/polystyrene/silica nanospheres via combined miniemulsion/emulsion polymerization. J Am Chem Soc 128(49):15582–15583

Xu Z, Hou Y, Sun S (2007) Magnetic core/shell Fe_3O_4/Au and Fe_3O_4/Au/Ag nanoparticles with tunable plasmonic properties. J Am Chem Soc 129:8698–8699

Xu C, Xie J, Ho D, Wang C, Kohler N, Walsh EG, Morgan JR, Chin YE, Sun S (2008) Au-Fe_3O_4 Dumbbell nanoparticles as dual functional probes. Angew Chem Int Ed 47:173–176

Yamazaki M, Ito M (1990) Deformation and instability in membrane-structure of phospholipid-vesicles caused by osmophobic association mechanical-stress model for the mechanism of poly(ethylene glycol)-induced membrane-fusion. Biochemistry 29(5):1309–1314

Yonezawa T, Yasui K, Kimizuka N (2001) Controlled formation of smaller gold nanoparticles by the use of four-chained disulfide stabilizer. Langmuir 17(2):271–273

Zhang Y, Kohler N, Zhang MQ (2002) Surface modification of superparamagnetic magnetite nanoparticles and their intracellular uptake. Biomaterials 23(7):1553–1561

Zhao MQ, Sun L, Crooks RM (1998) Preparation of Cu nanoclusters within dendrimer templates. J Am Chem Soc 120(19):4877–4878

Zhou WL, Carpenter EE, Lin J, Kumbhar A, Sims J, O'Conner CJ (2001) Nanostructures of gold coated iron core-shell nanoparticles and the nanobands assembled under magnetic field. Eur Phys J D 16(1–3):289–292